Journal of Materials Chemistry B

Accepted Manuscript

ROYAL SOCIETY OF CHEMISTRY

www.rsc.org/materialsB

Pascal Harimech,[1#] Raimo Hartmann,[1#] Joana Rejman,[1] Pablo del Pino,[2] Pilar Rivera Gil[1] and Wolfgang J. Parak[1,2*]

[1] Fachbereich Physik, Philipps Universität Marburg, Marburg, Germany
[2] CIC Biomagune, San Sebastian, Spain
[#] both authors contributed equally to this work
*corresponding author: wolfgang.parak@physik.uni-marburg.de

Encapsulated enzymes with integrated fluorescence-control of enzymatic activity

Abstract

A fluorescence-based particle sensor for oxaloacetic acid is presented. In the presence of nicotinamide adenine dinucleotide as cofactor, oxaloacetic acid is converted by malate dehydrogenase into L-malic acid. The reaction progress is monitored by sensing of proton consumption with an integrated pH sensor. The kinetics of this sensor is investigated on a single particle level. This work demonstrates the feasibility to detect analytes upon their enzymatic conversion into a product, which in turn can be sensed with a fluorophore responding to changes in the concentration of this product. Integration of enzymes and fluorophores into one carrier particle, as demonstrated here for the case of polyelectrolyte polymer capsules, allows to extend the range of analytes which can be detected with fluorescence, as it enhances selectivity. This coupled system allows to monitor enzymatic activity as well as kinetics of malate dehydrogenase.

Introduction

Analyte-sensitive fluorophores are common tools to measure the concentration of analytes in solution by means of fluorescence measurements.[1,2] Fluorophores which selectively respond to the presence of a large number of analytes have been reported in literature and many of them are also commercially available,[3,4] such as Ru(ddp), FluoZin, tetraphenylethene-based diboronic acid, $[Ru(phen)3]^{2+}$, *etc.*[1,2,5,6] Selectivity to the target analyte however is often limited, as the presence of other (similar) analytes triggers an unwanted crosstalk response. In addition, for many analytes no fluorophores, which show response upon their presence, has been described. One strategy to bypass these shortcomings is the use of enzymes. Enzymes are very selective to their target substrates. In case fluorophores responsive to the enzymatic product are used, analytes which serve as target for the enzyme can be selectively detected.[7-12] Ideally enzymes and fluorophores (in addition to organic fluorophores also quantum dots and luminescent metal nanoclusters have been used) should be coupled together into one entity, which is possible for example by linking both of them to colloidal particles. One convenient carrier particle system which allows for embedding analyte-sensitive fluorophores,[13-16] as well as enzymes,[17-24] are polyelectrolyte capsules fabricated by layer-by-layer assembly.[25-27] The walls of the capsules can be made semi-permeable which allows small analytes to diffuse inside the capsule to reach embedded fluorophores and enzymes, while retaining the fluorophores and enzymes inside the cavity of the capsule. In case fluorophores are not retained due to their small size they can be linked to larger molecules.[19] Combination of analyte-sensitive fluorophores and enzymes allows for selective detection of analytes/substrates.[28,29] For example, Kazakova *et al.* co-embedded urease and the pH-sensitive fluorophore seminaphtharhodafluor (SNARF) in polyelectrolyte capsules with the intention of designing an urea-selective fluorescence sensor.[29] Upon enzymatic processing of urea by urease, the local pH increases due to the production of ammonia, which is detected with the pH-sensitive fluorophore (*i.e.* consumption of protons). In principle, such enzyme-based fluorescence sensors could also be applied for intracellular sensing, similar to intracellular pH-sensing which has been demonstrated to monitor cellular reactions.[30] This would be in particular interesting for target molecules which are relevant for cellular function. Besides real-time determination of the intracellular concentrations of such target molecules, these capsules could be seen as theranostic devices. In case the concentration of an intracellular target is decreased by the enzymes delivered with the capsules, this decrease could be monitored directly by co-delivered fluorophores selective to one of the enzymatic products.

In this work a proof-of-concept of such an encapsulated enzyme-fluorophore couple for a biologically relevant target analyte is demonstrated. Specifically, we encapsulated malate dehydrogenase, an enzyme involved in many metabolic pathways, including the Krebs cycle, which reversibly converts oxaloacetic acid (OAA) into L-malic acid:

$$OAA + NADH + H^+ \rightleftharpoons \text{L-malic acid} + NAD^+$$

This reaction requires nicotinamide adenine dinucleotide (NADH) as a cofactor. During the enzymatic reaction protons are consumed/produced, depending on the direction of the

reaction. Based on the response of co-encapsulated pH-sensitive fluorophores SNARF-1 the reaction can be monitored by pH-sensing, *cf.* Figure 1. The kinetics of this combined system, in particular the one of its fluorescence read-out, is discussed in this work.

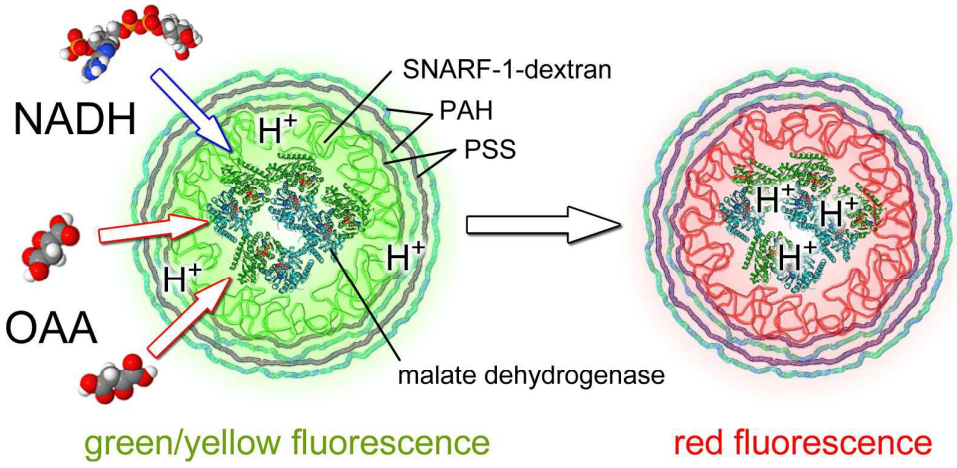

Figure 1. *Sensing principle: malate dehydrogenase and the pH-sensitive fluorescent dye SNARF-1-dextran are encapsulated inside hollow microcapsules made by deposition of alternating layers of polystyrene sulfonate (PSS) and poly(allylamine hydrochloride) (PAH). The presence of oxaloacetic acid (OAA) or nicotinamide adenine dinucleotide (NADH) inside the cavity can be sensed by SNARF-1-dextran in response to the local decrease in proton concentration caused by the enzymatic reaction OAA + NADH + H^+ → L-malic acid + NAD^+.*

Materials and Methods

Chemicals: Poly(sodium 4-styrenesulfonate) (PSS, $M_w \approx 70$ kDa, #243051), poly(allylamine hydrochloride) (PAH, $M_w \approx 56$ kDa, #283223), calcium chloride dehydrate ($CaCl_2$, #223506), sodium carbonate (Na_2CO_3, #S7795), ethylenediaminetetraacetic acid disodium salt dihydrate (EDTA disodium salt, #E5134), and malate dehydrogenase (#M2634) were purchased from Sigma-Aldrich (Germany). SNARF-1 dextran ($M_w \approx 70$ kDa, #D3304) from Life Technologies (Germany) was used. Sodium chloride (NaCl, #HN00.2), oxaloacetic acid (OAA, #4032.2), and β-nicotinamide adenine dinucleotide disodium salt (NADH, #AE12.1) were obtained from Roth (Karlsruhe, Germany). Phosphate buffered saline (PBS-Dulbecco, #L1825) was purchased from Biochrom (Berlin, Germany). Ultrapure double distilled water (ddH_2O) with a resistance greater than 18.2 MΩ cm^{-1} was used for all experiments.

Synthesis of polyelectrolyte sensor capsules: The synthesis of polyelectrolyte microcapsules (PEM) was carried out as described previously,[14,15,30,31] with the following modifications: $CaCO_3$ microparticles were prepared at room temperature (RT) from solutions of $CaCl_2$ and Na_2CO_3 under vigorous stirring in the presence of SNARF-1 dextran and malate

dehydrogenase. 615 µL of aqueous solution of $CaCl_2$ (0.33 M) with NaCl (1.33 M), 600 µL SNARF-1 dextran 70 kDa (1 mg mL^{-1}) and 100 µL malate dehydrogenase (11 mg protein mL^{-1}, 7700 U mL^{-1}) were mixed together in a glass vial. During magnetic stirring (1000 rpm) 615 µL of aqueous solution of Na_2CO_3 (0.33 M) with NaCl (1.33 M) solution was added quickly. After 30 s the stirrer was turned off and particle growth was stopped after additional 2 minutes by centrifugation. The particles were washed three times with ddH_2O and then directly used for the layer-by-layer assembly of polyelectrolytes. Alternating layers of negatively charged PSS (2 mg mL^{-1} in 0.5 M NaCl) and positively charged PAH (2 mg mL^{-1} in 0.5 M NaCl) were deposited onto the charged microparticles until four bilayers of polyelectrolytes had been established ($CaCO_3$@$(PSS/PAH)_4$). For coating with each layer the microparticles were suspended in 1 mL of polyelectrolyte solution, shaken gently for 10 minutes and washed three times with ddH2O. The dissolution of the cores was carried out by Ca^{2+} ion complexation with EDTA (1 mL, 0.2 M, pH 6) for several minutes. The resulting SNARF-1 and malate dehydrogenase containing microspheres were washed three times with ultrapure water to remove excess EDTA and stored at 4 °C. The size of the resulting capsules was ranging between 3 and 5 µm.

Fluorescence spectroscopy based sensing: To determine the response of SNARF-1 to the enzymatic activity of malate dehydrogenase in free solution a reaction mixture of 10 mM OAA, 75 µM NADH, 1 µL malate dehydrogenase (11 mg protein mL^{-1}, 7700 U mL^{-1}) and 100 µg mL^{-1} SNARF-1 was prepared. The pH of all stock solutions was adjusted to 6 with HCl and NaOH prior to use. Immediately after preparation SNARF-1 was excited at 540 nm with a FluoroLog (Horiba, Japan) fluorescence spectrometer and the emission was recorded over time between 560-700 nm.

Fluorescence microscopy based sensing: A confocal laser scanning microscope (cLSM) was used (LSM 510 Meta, Zeiss) for local sensing of pH-changes with polyelectrolyte sensor capsules. Drops of capsule solution were examined on a glass slide (approximately 40,000 capsules per drop of reaction mixture). SNARF-1 was excited simultaneously at 488 nm and 543 nm. The fluorescence signal was recorded at ranges between 550 – 615 nm (channel 1) and 615 – 750 nm (channel 2). The ratio of the fluorescence intensity of channel 2 (intensity I_r) / channel 1 (intensity I_y) was calculated for all pixel pairs where the intensity in both channels was above a threshold. The mean value for all pixel intensity ratios of one image (approximately 300 capsules) was calculated and used to determine the pH changes inside the capsule cavities caused by the enzymatic reaction catalyzed by malate dehydrogenase in the presence of the substrate OAA and the co-enzyme NADH. To determine reaction kinetics the fluorescence intensity of SNARF-1 in both channels was measured over time after addition of OAA and coenzyme consecutively, if not stated otherwise. Image processing was performed with Matlab (Mathworks). All solutions used for the experiments were adjusted to pH 6 with HCl or NaOH immediately before the sensing process was performed. The reaction mixture was buffered with PBS (5 %). The sensing experiments were always performed one day after capsules preparation.

Results and discussion

Four basic requirements have to be met in order to employ polyelectrolyte microcapsules for fluorescence sensing of products of enzymatic reactions. First, the enzymatic reaction itself should lead to a local change in concentration of free ions. Second, an ion-sensitive fluorophore-sensor should be loaded together with the catalytically active molecules (*i.e.* enzymes). Third, the molecular size of the dye and the catalyst should be sufficiently large to retain them within the capsule cavity. Last, substrate molecules should be small enough to penetrate through the capsule wall. Hereby, the precise molecular weight cut-offs depend on the capsule material and architecture.

In our experimental set-up we evaluated sensing capacities of microcapsules carrying malate dehydrogenase (70 kDa, isoelectric point: 10) and the pH-sensitive dye SNARF-1. SNARF-1 was coupled to dextran (70 kDa) to increase the molecular size of the fluorescent probe and to ascertain that it is retained inside the capsule cavity.[15] The maximum of the emission spectrum of SNARF-1 shifts from 580 nm in acidic media to 640 nm in alkaline media. As described, the pK_a of the fluorophore might change in different environments. While the pK_a of the free dye is in accordance with the manufacturer's value of 7.50, it changes when encapsulated,[15,29] in the present case while encapsulated together with malate dehydrogenase to about 6.80.

Malate dehydrogenase is an enzyme of the citric acid cycle. The molecular weight of the enzyme (70) kDa is sufficient to keep it inside the cavity. The conversion of L-malic acid into oxaloacetic acid is catalysed by the enzyme. This is accompanied by the reduction of the cofactor NAD^+ into NADH and the release of one hydrogen ion per each reaction. The reaction constant of the enzyme depends on the concentration of the respective substrate as well as on the pH of the solution. Depending on the initial conditions the reaction can proceed in both directions. In case of low pH-values (*i.e.* when many protons are available) and low concentration of L-malic acid the reaction runs to the right, protons are consumed, and thus the local pH increases (*cf.* Figure 1a): OAA + NADH + $H^+ \rightarrow$ L-malic acid + NAD^+. In case of high pH values the reaction rather runs to the left, protons are produced, and thus the local pH decreases: OAA + NADH + $H^+ \leftarrow$ L-malic acid + NAD^+. Note that SNARF-1 is only sensitive to changes in pH around its pK_a value, and thus this fluorophore can be used to monitor the reaction in a certain pH range only. The reverse reaction OAA + NADH + $H^+ \leftarrow$ L-malic acid + NAD^+ is favoured in the region were SNARF-1 most strongly responds to changes in pH.

In order to verify that the reaction ensures a significant impact on the pH, we first tested the reaction using free substrate (OAA), free cofactor (NADH), free enzyme (malate dehydrogenase), and free SNARF-1-dextran as pH indicator in solution of initial pH = 6. Upon adding the substrate (10 mM OAA) and the cofactor (75 μM NADH) to the enzyme (7700 units/mL) a time-dependent change of fluorescence signal of the solution from dominant emission in the yellow (580 nm) to dominant emission in the red (640 nm) was observed which indicates that upon consumption of protons the solution became more

alkaline, *cf.* Figure 2a. A calibration curve which allows obtaining the pH from the ratio of red-to-yellow fluorescence (I_r/I_y) is shown in Figure 2b. These data demonstrate that the reaction catalysed by malate dehydrogenase can be monitored *in situ* by accompanied monitoring of pH.

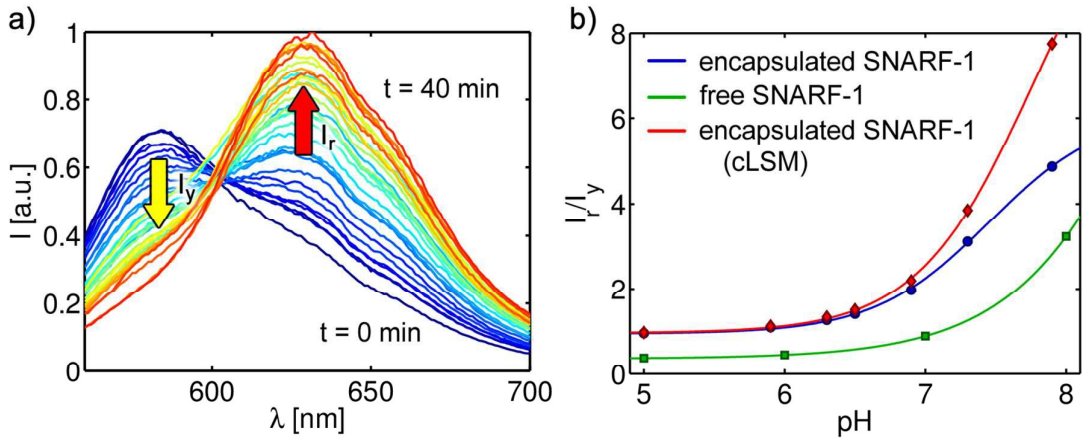

Figure 2. *a) Changes in the emission spectra of free SNARF-1-dextran in a solution (initial pH = 6) of OAA (10 mM) and NADH (75 µM) and malate dehydrogenase in response to malate dehydrogenase activity. The emission of free SNARF-1-dextran shifts from the yellow (intensity I_y) to the red (intensity I_r) region, indicating a continuos increase in pH (after 40 min pH = 7.4). This is the result of proton consumtion in the reaction OAA + NADH + H^+ → L-malic acid + NAD^+. b) Comparision of the response I_r/I_y(pH) for free and encapsulated SNARF-1 dextran as obtained by spectrofluorimetry (blue and green curve) and cLSM (red).*

In addition to the fluorescent pH indicator SNARF-1-dextran also the pH indicator thymol blue was utilized, whose absorption spectrum changes in response to pH. Using UV/vis absorption spectroscopy allowed for measuring pH during the reaction (by monitoring changes in the spectrum of thymol blue), in addition to directly measuring changes in the NADH concentration. Thymol blue changes its colour from blue (pH > 9) to yellow (pH < 7.4) (*cf.* Figure S1). The visual change is attributed to an increase in absorption at 430 nm and a decrease at 595 nm (*cf.* Figure S2). The change in absorption at 595 nm is more sensitive and shows the sigmoidal slope typical for a pH indicator. In contrast, the cofactor NADH shows two absorption bands at 260 nm and 340 nm, whilst the oxidized form NAD^+ absorbs only at 260 nm. Therefore, we analysed the change in NADH concentration in the solution by UV/vis absorption spectroscopy at 340 nm. This method is common in systems involving NAD^+/NADH for the determination of enzyme activities. These measurements cannot be performed in the presence of the dye, because of its absorption in the UV. The full set of data using UV/vis absorption spectroscopy is presented in the SI. In agreement with experiments involving SNARF-1-dextran the data verify that the enzymatic activity of malate dehydrogenase can be followed by *in situ* pH measurements, in which a pH indicator and an enzyme are free in solution.

For the construction of a sensor system we attempted to link both the enzyme and the pH-sensitive dye into one carrier particle. As there are multiple molecules in solution (in

particular the carrier particles which absorb and scatter light) we decided to use fluorescence instead of absorption spectroscopy as most convenient read-out, and employed SNARF-1-dextran as a pH-sensitive reporter. Polyelectrolyte polymer capsules fabricated by layer-by-layer assembly were used as microreactor particles. To prepare the sensing microcapsules, malate dehydrogenase and SNARF-1-dextran were first co-precipitated in calcium carbonate particles. The particles were then coated with PSS and PAH using the well-described layer-by-layer technique.[32-34] In a final step the $CaCO_3$ template was removed by re-dispersing the capsules in EDTA, which forms complexes with the Ca^{2+} ions. The resulting capsules filled with the enzyme and SNARF-1-dextran had a diameter of 3-5 μm. An image of such capsules is presented in Figure 3. The capsules were spherical and well dispersed. The fluorescent dye SNARF-1-dextran was encapsulated and remained within the capsule after removal of the core. As reported in previous studies the dye is not homogeneously distributed in the capsule cavity, rather sticking to the inner capsule wall.[15] Because SNARF-1 molecules were coupled to 70 kDa dextran, which has the same molecular weight as the enzyme, it is reasonable to assume that the enzyme stays within the cavity as well, in agreement with previous studies,[19] though its presence cannot be concluded from the microscopy images.

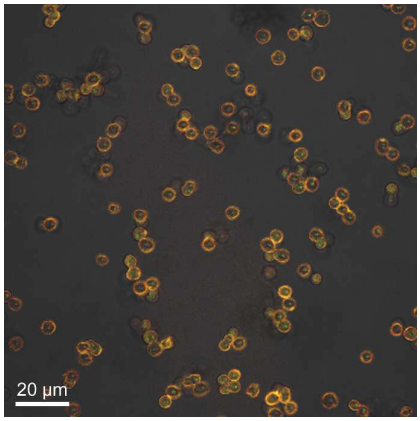

Figure 3. *Fluorescent micrograph of sensor capsules. An overlay of the transmission and fluorescence channels (recorded with a cLSM) is shown in false colours (green: 560-615 nm, red: 615 – 750 nm). The scale bar corresponds to 20 μm.*

Finally, we examined the combined system (enzyme and SNARF encapsulated together) by recording the fluorescence intensities of SNARF-1-dextran at suitable wavelengths using a fluorescence microscope. The presence and activity of the enzyme can be proven by recording the changes in pH. Controls with capsules without the enzyme were first investigated. *cf.* Figure 4. The presence of the cofactor NADH has no impact on the I_r/I_y-read out of the dye, *cf.* Figure 4A. Although in this case no enzymatic conversion can take place due to the lack of the enzyme OOA already interacts with SNARF-1 as seen by increasing I_r/I_y-values over time, independent on whether NADH is present or not, *cf.* Figure 4B-C. OOA slowly decomposes in aqueous solution into pyruvic acid and CO_2 accompanied by an increase in pH. Though, the rate of the alkalinizing effect of this decomposition was determined to be much slower than the observed phenomenon in Figure 4B-C.

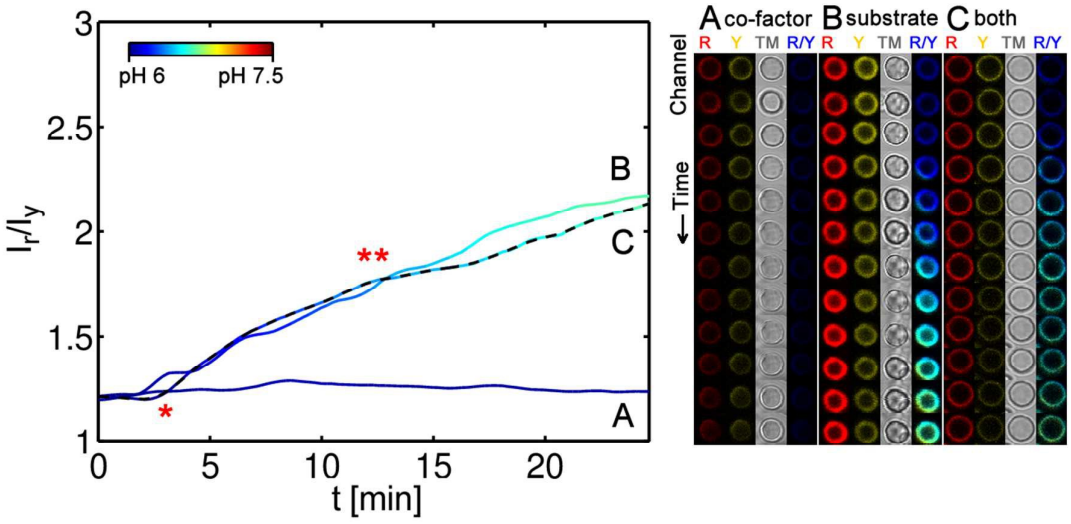

Figure 4. *Control system. Polyelectrolyte multilayer capsules without malate dehydrogenase were prepared. The capsules carrying SNARF-1-dextran only were exposed to OAA (500 µM) in the absence (B) or in the presence of NADH (50 µM, C, dashed line). Lane A represents results obtained for the cofactor alone (500 µM). The substrate (OAA) was added at the time point indicated with an asterisk. The cofactor (NADH) was added at the time point marked with two asterisks. The reaction was followed for 25 minutes. The initial pH of all solutions was adjusted to 6. Corresponding fluorescence images are shown on the right side illustrating the response of a single capsule in the red (R) and yellow (Y) channel, in brightfield transmission mode (TM) and in a pseudo-coloured image (R/Y) corresponding to the ratio I_r/I_y per pixel (same colourmap as used in the plot window). Correlation of I_r/I_y. to pH is shown in Figure 2b, and is indicated by the colour code presented in the top panel.*

In the next set of experiments capsules carrying malate dehydrogenase were exposed to their substrate OAA, in the presence of different concentrations of the cofactor NADH. The changes in SNARF-1-dextran fluorescence intensities were then recorded. As shown in Figure 5 the initiation of the enzymatic reaction led to a decrease in the amount of free H^+ ions. This was visualised by the change in the ratio I_r/I_y of the fluorescence intensities of SNARF-1-dextran as recorded in the range from 560-615 nm (I_y, yellow channel) to 615 – 750 nm (I_r, red channel), *cf.* Figure 2a. The reaction only took place in case of presence of the substrate (OAA). Without the substrate the pH of the solution remained constant over time (*cf.* Figure 5A), indicating that no reaction occurred. Presence of cofactor increased the reaction rate. Saturation at high I_r/I_y-values is caused by a decrease of the reaction rate and not by limited sensitivity of SNARF-1 as at $I_r/I_y > 3.5$ SNARF-1 is still responsive to changes in pH, *cf.* Figure 2b.

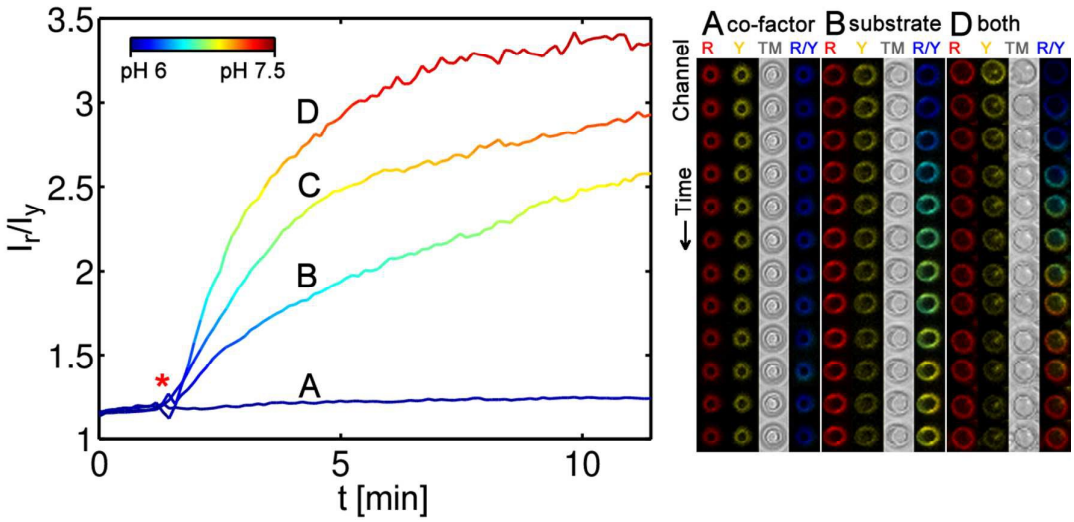

Figure 5. *Concentration-dependent changes in the emission spectra I(λ) of encapsulated SNARF-1-dextran, reported as $I_r/I_y(t)$, in response to malate dehydrogenase activity. The sensor capsules carrying malate dehydrogenase and SNARF-1-dextran were exposed to OAA (500 µM) in the absence (B) or in the presence of NADH (50 µM (C) or 100 µM (D)). The substrate and the cofactor were added at the time point indicated with an asterisk. Lane A represents results obtained for the cofactor alone (500 µM). The reaction was followed for 12 min. The initial pH of all solutions was adjusted to 6. Corresponding fluorescent images are shown on the right side illustrating the response of a single capsule in the red (R) and yellow (Y) channel, in brightfield transmission mode (TM) and in a pseudo-coloured image (R/Y) corresponding to the ratio I_r/I_y per pixel (same colourmap as used in the plot window). The I_r/I_y ratio could be directly related in corresponding pH values according to Figure 2b, as displayed by the colour code in the panel.*

To demonstrate the effect of the cofactor on the kinetics of the enzymatic reaction, the capsules carrying the enzyme were incubated with the substrate first, followed by the addition of NADH. As shown in Figure 6, the more coenzyme was added, the higher was the increase in fluorescence intensities of SNARF-1 in the red channel. Moreover, the sensor capsules showed no significant response to the cofactor alone (*cf.* Figure 6A). Addition of the substrate caused a steady increase of the I_r/I_y ratio (*cf.* Figure 6B) as already seen for the control particles without encapsulated enzymes, *cf.* Figure 4B. The reaction could be enhanced by addition of NADH (*cf.* Figure 6C-E *versus* Figure 6B). At initial NADH concentration of 100 µM the local pH strongly increased temporarily (*cf.* Figure 6C-D). After a few minutes the cofactor was used up and the pH inside the capsules got equilibrated with the outside value. For higher concentrations of the cofactor also the bulk pH was increased by the sensing reaction (*cf.* Figure 6E). Note that the I_r/I_y curves with OAA and with NADH lie on top of the curve with OAA, but without NADH. In case of small amounts of NADH added (*cf.* Figure 6C), after NADH has been consumed by the enzymatic reaction, the I_r/I_y curve approaches the curve in which NADH was not added (*cf.* Figure 6B). Only in case the cofactor is present the substrate can be enzymatically converted.

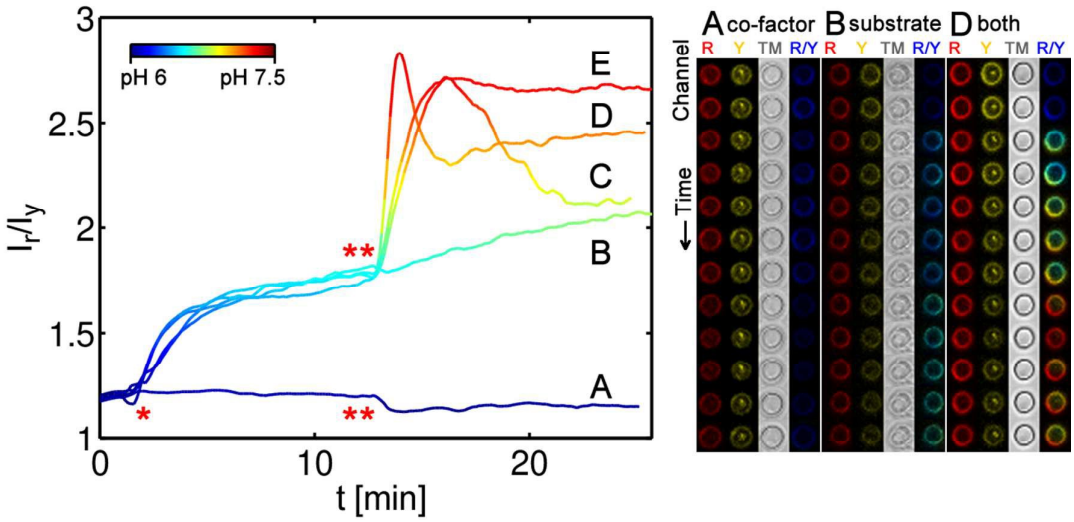

Figure 6. *Reaction kinetics - response of sensor capsules to different concentrations of substrate and cofactor. The sensor capsules carrying malate dehydrogenase and SNARF-1-dextran were exposed to different concentrations of OAA and NADH. A - NADH (200 µM); B - OAA (350 µM); C - OAA (350 µM) + NADH (100 µM); D - OAA (700 µM) + NADH (100 µM); E- OAA (350 µM) + NADH (200 µM). The substrate (OAA) was added at the time point indicated with an asterisk. The cofactor (NADH) was added at the time point marked with two asterisks. The reaction was followed for 25 minutes. The initial pH of all solutions was adjusted to 6. Corresponding fluorescent images are shown on the right side illustrating the response of a single capsule in the red (R) and yellow (Y) channel, in brightfield transmission mode (TM) and in a pseudo-coloured image (R/Y) corresponding to the ratio I_r/I_y per pixel (same colourmap as used in the plot window).*

The data in Figure 6C-D suggest that the continuance of the enzymatic reaction is limited by the amount of NADH present. Therefore, we tested whether it could be continued by supplying the system with additional NADH. To that end the sensing capsules carrying malate dehydrogenase were first incubated with the substrate, followed by the addition of the cofactor. When the I_r/I_y ratio was reaching a plateau value, additional NADH was added. Indeed, as seen in Figure 7, this allowed the reaction to be continued.

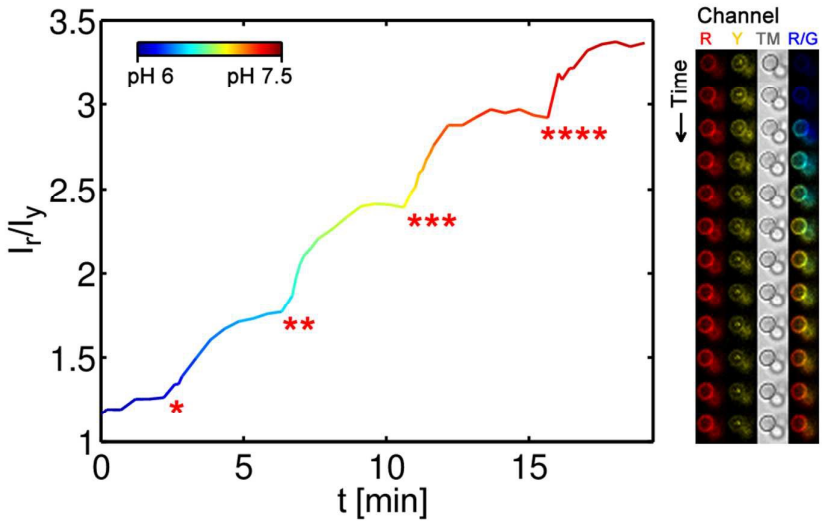

Figure 7. *Reaction kinetics – response of sensor capsules to step-wise addition of cofactor. At (*) the substrate was added to the capsule solution to obtain an initial concentration of 500 µM (total volume: 50L). Subsequently 1 µL of cofactor solution (350 µM) was added at each step (**)-(****).The initial pH of all solutions was adjusted to 6. Corresponding fluorescent images are shown on the right side illustrating the response of a single capsule in the red (R) and yellow (Y) channel, in brightfield transmission mode (TM) and in a pseudo-coloured image (R/Y) corresponding to the ratio I_r/I_y per pixel (same colourmap as used in the plot window).*

Conclusions

The synthesis and characterization of a particle bound sensor for the detection of OAA, based on enzymatic digestion followed by pH measurements has been demonstrated. As enzymatic conversion of OAA is a continuous process, as long as substrate and cofactor are available, this reaction needs to be monitored over time. This has been demonstrated with time lapse recordings of individual polyelectrolyte capsules, which serve as carrier particles for both, enzymes and pH sensitive fluorophores. As the present work was a proof-of-concept study no detailed analysis about selectivity and sensitivity is given. Instead it is interesting to discuss the potential applications of such sensors for intracellular detection. It is well accepted that polyelectrolyte polymer capsules as used here are internalized by adherent cell lines *via* endocytosis, and that their final intracellular location is the lysosome.[31,35-37] This however involves general problems associated with particle based intracellular sensing.[16] Though some methods exist to release molecules from capsules (in the size range from ca. 150 nm[38] to 3-5 µm[39-41]) residing inside lysosomes into the cytosol, in a typical scenario sensors will remain trapped inside lysosomes, which suggests sensing in the lysosome as most facile application. Besides imposing a hostile environment to particles (lysosomal proteases, highly acidic pH), localization inside the lysosome imposes other limits to particle based intra-lysosomal sensing. The sensing principle as sketched in Figure 1 relies on the detection of protons, which are consumed upon enzymatic digestion of the target molecule OAA. However, all pH-

sensitive fluorophores have a limited range of operation, centred along their pK_a value. While the lysosomal pH can be highly acidic down to pH values of 3 (precise values depend on the cell line), the pK_a value of encapsulated SNARF-1-dextran as used in this study is 6.8. Thus, inside lysosome the pH-indicator SNARF-1 would be barely sensitive to small changes in pH upon digestion of OAA by malate dehydrogenase. In the data shown in this work the pH of the starting solution was buffered on purpose to a value around 6, which sets an optimal range for observing increase in pH upon the enzymatic reaction. In order to apply the sensing strategy for intra-lysosomal detection of OAA, an alternative pH-indicator with highly acidic pK_a value would be required. In the Supporting Information thymol blue is presented as an example in this direction, though its pK_a value (*ca.* 1.7) would be too low for sensing inside the lysosomes. It also needs to be pointed out, that the particle architecture could be improved. In our work enzymes and analyte-sensitive fluorophores were co-localized in the cavity of polyelectrolyte polymer capsules. However, these capsules in principle also allow for a multicompartment-structure, in which enzymes and fluorophores could be placed at different locations.[42-47] Based on these considerations we suggest that further improvements could help to facilitate intracellular enzyme-based fluorescence sensing using polymer capsules as carrier systems. In addition to intracellular sensing, other potential applications which involve enzymatic or enzymatic-coupled reactions could be envisioned, such as enzymatic microreactors for chemical analysis (e.g. sensing of glucose, food contaminants, etc.), kinetic studies and catalysis. At any rate, it should be highlighted that inhomogeneous and/or variable loading of molecules in the capsules, as well as different diffusion limits of the molecules involved, hampers the application of the current coupled system for absolute detection of concentrations (be it for the proof-of-concept system described here or be it for other enzyme-based sensing system). Nevertheless, here the reported proof-of-concept system demonstrates the feasibility of real time monitoring of enzymatic reactions (as well as kinetics) *in situ*. Further material's improvements (e.g. homogeneous loading, development of new fluorescence probes, multi-compartmental geometries, etc.) will strengthen the potential applications of enzyme-loaded capsules.

Acknowledgements

This work was supported by LOEWE (grant Synchembio to WJP).

References

1. D. W. Domaille, E. L. Que and C. J. Chang, *Nat Chem Biol*, 2008, **4**, 168-175.
2. L. Kazakova, L. Shabarchina, S. Anastasova, A. Pavlov, P. Vadgama, A. Skirtach and G. Sukhorukov, *Anal Bioanal Chem*, 2013, **405**, 1559-1568.
3. A. S. Susha, A. Munoz_Javier, W. J. Parak and A. L. Rogach, *Colloids And Surfaces A-Physicochemical And Engineering Aspects*, 2006, **281**, 40-43.
4. M. J. Ruedas-Rama, A. Orte, E. A. H. Hall, J. M. Alvarez-Pez and E. M. Talavera, *Analyst*, 2012, **137**, 1500-1508.
5. W. Qi, Z. Liu, J. Lai, W. Gao, X. Liu, M. Xu and G. Xu, *Chemical Communications*,

2014, **50**, 8164-8166.
6. E. A. Lemke and C. Schultz, *Nat Chem Biol*, 2011, **7**, 480-483.
7. M. J. Ruedas-Rama and E. A. H. Hall, *Analytical Chemistry*, 2010, **82**, 9043-9049.
8. V. Pavlov, B. Shlyahovsky and I. Willner, *Journal of the American Chemical Society*, 2005, **127**, 6522-6523.
9. R. Freeman and I. Willner, *Nano Letters*, 2009, **9**, 322-326.
10. R. Freeman, L. Bahshi, T. Finder, R. Gill and I. Willner, *Chemical Communications*, 2009, 764-766.
11. F. Khan, T. E. Saxl and J. C. Pickup, *Analytical Biochemistry*, 2010, **399**, 39-43.
12. F. Wen, Y. Dong, L. Feng, S. Wang, S. Zhang and X. Zhang, *Analytical Chemistry*, 2011, **83**, 1193-1196.
13. S. Hiller, A. Schnackel and E. Donath, *Cytometry Part A*, 2005, **64A**, 119-119.
14. M. Semmling, O. Kreft, A. Muñoz Javier, G. B. Sukhorukov, J. Käs and W. J. Parak, *Small*, 2008, **4**, 1763-1768.
15. L. L. del Mercato, A. Z. Abbasi and W. J. Parak, *Small*, 2011, **7**, 351-363.
16. K. Kantner, S. Ashraf, S. Carregal-Romero, C. Carrillo-Carrion, M. Collot, P. del Pino, W. Heimbrodt, D. J. De Aberasturi, U. Kaiser, L. I. Kazakova, M. Lelle, N. M. de Baroja, J. M. Montenegro, M. Nazarenus, B. Pelaz, K. Peneva, P. R. Gil, N. Sabir, L. M. Schneider, L. I. Shabarchina, G. B. Sukhorukov, M. Vazquez, F. Yang and W. J. Parak, *Small*, 2014, DOI: 10.1002/smll.201402110, n/a-n/a.
17. O. P. Tiourina, A. A. Antipov, G. B. Sukhorukov, N. L. Larionova, Y. Lvov and H. Mohwald, *Macromolecular Bioscience*, 2001, **1**, 209-214.
18. N. G. Balabushevich, G. B. Sukhorukov and N. I. Larionova, *Macromol. Rapid Commun.*, 2005, **26**, 1168-1172.
19. M. Ochs, S. Carregal-Romero, J. Rejman, K. Braeckmans, S. C. De Smedt and W. J. Parak, *Angew. Chem. Int. Ed.*, 2013, **52**, 695-699
20. C. S. Karamitros, A. M. Yashchenok, H. Moehwald, A. G. Skirtach and M. Konrad, *Biomacromolecules*, 2013, **14**, 4398-4406.
21. F. Caruso, D. Trau, H. Möhwald and R. Renneberg, *Langmuir*, 2000, **16**, 1485-1488.
22. M. Fischlechner, Y. Schaerli, M. F. Mohamed, S. Patil, C. Abell and F. Hollfelder, *Nat Chem*, 2014, **6**, 791-796.
23. A. M. Pavlov, G. B. Sukhorukov and D. J. Gould, *Journal of Controlled Release*, 2013, **172**, 22-29.
24. O. S. Sakr and G. Borchard, *Biomacromolecules*, 2013, **14**, 2117-2135.
25. E. Donath, G. B. Sukhorukov, F. Caruso, S. A. Davis and H. Möhwald, *Angew. Chem. Int. Ed.*, 1998, **37**, 2202-2205.
26. G. B. Sukhorukov, A. L. Rogach, B. Zebli, T. Liedl, A. G. Skirtach, K. Köhler, A. A. Antipov, N. Gaponik, A. S. Susha, M. Winterhalter and W. J. Parak, *Small*, 2005, **1**, 194-200.
27. M. F. Bedard, A. Munoz-Javier, R. Mueller, P. del Pino, A. Fery, W. J. Parak, A. G. Skirtach and G. B. Sukhorukov, *Soft Matter*, 2009, **5**, 148-155.
28. O. Kreft, M. Prevot, H. Mohwald and G. B. Sukhorukov, *Angew Chem Int Ed Engl*, 2007, **46**, 5605-5608.
29. L. I. Kazakova, L. I. Shabarchina and G. B. Sukhorukov, *Physical Chemistry*

Chemical Physics, 2011, **13**, 11110.
30. P. Rivera Gil, M. Nazarenus, S. Ashraf and W. J. Parak, *Small*, 2012, **8**, 943-948.
31. R. Hartmann, M. Weidenbach, M. Neubauer, A. Fery and W. J. Parak, *Angew. Chem. Int. Ed.*, 2014, DOI: 10.1002/anie.201409693, n/a-n/a.
32. P. Rivera Gil, L. L. del Mercato, P. del Pino, A. Muñoz-Javier and W. J. Parak, *Nano Today*, 2008, **3**, 12-21.
33. J. W. Cui, M. P. van Koeverden, M. Mullner, K. Kempe and F. Caruso, *Adv. Colloid Interface Sci.*, 2014, **207**, 14-31.
34. S. De Koker, R. Hoogenboom and B. G. De Geest, *Chemical Society Reviews*, 2012, **41**, 2867-2884.
35. A. Muñoz_Javier, O. Kreft, M. Semmling, S. Kempter, A. G. Skirtach, O. Bruns, P. d. Pino, M. F. Bedard, J. Rädler, J. Käs, C. Plank, G. Sukhorukov and W. J. Parak, *Advanced Materials*, 2008, **20**, 4281-4287.
36. L. Kastl, D. Sasse, V. Wulf, R. Hartmann, J. Mircheski, C. Ranke, S. Carregal-Romero, J. A. Martínez-López, R. Fernández-Chacón, W. J. Parak, H.-P. Elsaesser and P. Rivera Gil, *ACS Nano*, 2013, **7**, 6605-6618
37. Y. Yan, A. P. R. Johnston, S. J. Dodds, M. M. J. Kamphuis, C. Ferguson, R. G. Parton, E. C. Nice, J. K. Heath and F. Caruso, *ACS Nano*, 2010, **4**, 2928-2936.
38. J. Ruesing, O. Rotan, C. Gross-Heitfeld, C. Mayer and M. Epple, *Journal of Materials Chemistry B*, 2014, **2**, 4625-4630.
39. A. Muñoz Javier, P. del Pino, M. F. Bedard, A. G. Skirtach, D. Ho, G. B. Sukhorukov, C. Plank and W. J. Parak, *Langmuir*, 2008, **24**, 12517-12520.
40. S. Carregal-Romero, M. Ochs, P. Rivera Gil, C. Ganas, A. M. Pavlov, G. B. Sukhorukov and W. J. Parak, *Journal of Controlled Release* 2012, **159**, 120-127.
41. C. Ganas, A. Weiß, M. Nazarenus, S. Rösler, T. Kissel, P. Rivera_Gil and W. J. Parak, *J. Control. Release*, 2014, **196**, 132-138.
42. O. Kreft, A. G. Skirtach, G. B. Sukhorukov and H. Mohwald, *Advanced Materials*, 2007, **19**, 3142-+.
43. L. L. del Mercato, A. Z. Abbasi, M. Ochs and W. J. Parak, *ACS Nano*, 2011, **5**, 9668-9674.
44. B. V. Parakhonskiy, A. M. Yashchenok, M. Konrad and A. G. Skirtach, *Adv. Colloid Interface Sci.*, 2014, DOI: 10.1016/j.cis.2014.1001.1022.
45. R. Xiong, S. J. Soenen, K. Braeckmans and A. G. Skirtach, *Theranostics*, 2013, **3**, 141-151.
46. M. Delcea, H. Moehwald and A. G. Skirtach, *Adv. Drug Delivery Rev.*, 2011, **63**, 730-747.
47. M. Delcea, A. Yashchenok, K. Videnova, O. Kreft, H. Möhwald and A. G. Skirtach, *Macromolecular Bioscience*, 2010, **10**, 465.

TOC: Capsules filled with enzymes and fluorescence-probes allows to monitor in situ enzymatic activity as well as kinetics on a single particle level.